PAPER

Fabrication of silver nanostructures using femtosecond laser-induced photoreduction

IOP Publishing Nanotechnology
Nanotechnology 28 (2017) 505302 (8pp) https://doi.org/10.1088/1361-6528/aa977b

Fabrication of silver nanostructures using femtosecond laser-induced photoreduction

Peter Barton[1], Sanjoy Mukherjee[2], Jithin Prabha[1], Bryan W Boudouris[2,3], Liang Pan[1] and Xianfan Xu[1]

[1] School of Mechanical Engineering and Birck Nanotechnology Center, Purdue University, West Lafayette, IN 47906, United States of America
[2] Charles D. Davidson School of Chemical Engineering, Purdue University, West Lafayette, IN 47907, United States of America
[3] Department of Chemistry, Purdue University, West Lafayette, IN 47907, United States of America

E-mail: xxu@ecn.purdue.edu

Received 4 September 2017, revised 20 October 2017
Accepted for publication 1 November 2017
Published 23 November 2017

Abstract

Silver nanostructures were fabricated by femtosecond laser-induced reduction of silver ions and the impact of solution chemistry on the fabricated structures was evaluated. By investigating the exact photochemistry of the nanofabrication solutions, which contained varying amounts of diamine silver ions, trisodium citrate, and n-lauroylsarcosine sodium, and optimizing the laser processing parameters, we fabricated two-dimensional silver pads with surface roughness values of 7 nm and stable 2.5-dimensional shell structures with heights up to 10 μm and aspect ratios of 20 in a ready manner. Moreover, thermal annealing of these structures afforded materials where the average resistivity value was only a factor of 4 greater than that of bulk silver. In this way, the work presented here provides for a methodology that can be used for laser direct fabrication of metal nanostructures for applications in plasmonics and micro- and nano-electronics.

Keywords: laser fabrication, metal nanostructure, photoreduction

(Some figures may appear in colour only in the online journal)

1. Introduction

Implementing multiphoton lithography in the fabrication of nanostructures has generated much research interest in the past two decades because of the key advantages this technique has over other forms of lithography, e.g., fabrication resolutions below the diffraction limit of light and flexible patterning without the need for expensive photomasks. Much of the previous work in the field uses a photoresist as the fabrication medium, and this results in polymer-based structures [1–4]. While these polymer structures can be used for many applications (e.g., microfluidic devices), diversifying the materials portfolio to include metallic structures is a requirement for other applications such as electronic and plasmonic elements. Fortunately, it is possible to fabricate metallic micro- and nanostructures using multiphoton absorption through the photoreduction of metal ions, which was first reported in 1976 [5]. Additional agents can be added to increase the quantum yield of photoreduction and reduce the size of fabricated metal parts [6].

In a similar manner to two-photon polymerization, when the incident light intensity reaches a critical value, molecules in metal ionic solution can undergo two-photon absorption to reduce the metal ions. This was first shown using an ultrafast laser [7]. In this case, aqueous silver nitrate was added to a sol–gel matrix and an 800 nm ultrafast laser was used to reduce the silver ions to silver metal. The resulting structures consisted of three-dimensional discontinuous patterns of silver nanoparticles suspended inside a dielectric matrix. Since this groundbreaking effort, most reports using two-photon reduction fabrication have been centered upon the reduction of silver ions inside of a dielectric matrix [8–15]. However, this is not an ideal design paradigm for microelectronic applications as the resulting structures often have a large electrical resistivity and are not mechanically stable if the dielectric matrix is removed. Thus, a variation of the two-photon reduction fabrication method was

Table 1. Summary of all fabrication solutions used in this manuscript.

Fabrication solution number	Fabrication solution contents	Chemical formula
1	Diammine silver ions (DSI)	$H_2O + [Ag(NH_3)_2]^+$
2	DSI + N-lauroylsarcosine sodium (NLSS)	$H_2O + [Ag(NH_3)_2]^+ + C_{15}H_3NNaO_3$
3	DSI + trisodium citrate	$H_2O + [Ag(NH_3)_2]^+ + Na_3C_6H_5O_7$
4	DSI + NLSS + trisodium citrate	$H_2O + [Ag(NH_3)_2]^+ + C_{15}H_3NNaO_3 + Na_3C_6H_5O_7$

developed, and this technique uses a liquid solution of metal ions as the fabrication medium and a metallic film as the deposition substrate [16–20]. In this method, when the laser is focused at the substrate surface, the metal ions are reduced to silver atoms and/or nanoparticles that are then deposited onto the substrate. This allows for arbitrary two-dimensional patterns to be created on the surface, and three-dimensional structures can then be fabricated by raising the focal spot and scanning the laser on the previously deposited metal.

While implementing this method in the absence of protecting agents has allowed for wires to be fabricated with only a factor of 3.3× increase in the resistivity of the deposited silver relative to the bulk, submicron regime patterning could not be achieved, and the three-dimensional structures generated had large surface roughness values [16]. As such, an ionic surfactant, n-lauroylsarcosine sodium (NLSS) salt, was added to the deposition bath, and this resulted in much smoother nanowires with a resolution of 120 nm and three-dimensional structures with 180 nm resolution [18]. It was hypothesized that the large size of these surfactant molecules would result in nanowires with large resistivity, so the smaller surfactant-like citrate molecule was used and the resulting nanowires had resistivity of 10× that of bulk silver [20].

The current limitations of fabricating metal nanostructures using this method that need to be addressed include the low mechanical stability of fabricated structures with heights greater than a few microns, the rough surface topology of fabricated three-dimensional structures, and the large resistivity of the fabricated nanowires while maintaining submicron linewidth. In order to address these issues, we investigate the photochemistry associated with the nanofabrication solutions that contain varying amounts of diamine silver ions (DSIs), trisodium citrate, and NLSS salt. By systematically varying the composition of the deposition bath and optimizing the laser processing parameters, we are able to fabricate high-fidelity 2D and 2.5D structures using these chemical solutions in a straightforward manner. Importantly, optimization of the deposition bath conditions with respect to the concentrations of trisodium citrate and the long-chain surfactant allowed us to increase the surface quality and mechanical stability of fabricated two and three-dimensional structures. Moreover, the average resistivity of the fabricated structures was only 4-fold relative to that of bulk silver. Square silver pads of 7 nm surface roughness were fabricated as well as three-dimensional shell structures with a height-to-width aspect ratio of 20. These results show it is possible to achieve silver nanostructures with high aspect ratios that can be used to readily fabricate microelectronic devices. Furthermore, submicron silver wires were fabricated with low resistivity using this method, which provides a simpler alternative to photolithography for fabricating microcircuitry.

2. Experimental

The ultrafast laser used for delivering the incident photons was a Coherent Micra-10 operating at an 800 nm central wavelength with a 23 fs pulse width and 80 MHz repetition rate. An oil emersion 100× objective lens with a N.A. of 1.49 was used to focus the beam to the substrate, which was fitted to an inverted microscope. A computer controlled tip-tilt mirror was used to control the beam scanning in the orthogonal in-plane (x- and y-) directions and a computer controlled piezo-objective scanner was used to scan the beam in the out-of-plane (z-) direction.

All stock solutions used for the studies were prepared using ultrapure water as the solvent throughout all the experiments. $AgNO_3$ and trisodium citrate were purchased from Alfa Aesar and n-lauroylsarcosine sodium salt (NLSS) was purchased from Sigma Aldrich. Dropwise addition of aqueous ammonia (NH_3) to a aqueous solution of $AgNO_3$, resulted in the formation of a clear solution of $[Ag(NH_3)_2]^+NO_3^-$ (after the initial formation of an insoluble Ag_2O species). This solution was used as a stock to prepare other solutions containing the NLSS surfactant and the reducing agent (trisodium citrate). All the solutions were stored in amber colored vials in the dark to prevent any unintended photoreactions from occurring. Then, a single drop of the solution was drop cast between two borosilicate glass cover slips with Scotch tape (nominal thickness of ~100 μm) serving as the spacer. The solution drops initially are taller than 100 μm, so when the top cover slip is placed the solution thickness is 100 μm. Subsequently, the nanostructures were fabricated by first scanning the bottom layer on the upper cover slip and lowering the focal height for subsequent layers. After fabrication, the cover slip was rinsed in the fabrication solution to dissolve any dried material, then rinsed in water and dried with nitrogen. Table 1 summarizes all fabrication solutions used.

Ultraviolet–visible (UV–vis) light absorption spectroscopy data were acquired on a Cary 60 spectrometer over a wavelength range of $300 \leqslant \lambda \leqslant 800$ nm. Solutions were placed in quartz cuvettes with 1 cm path lengths for data collection. The fabricated structures were characterized using scanning electron microscopy (SEM) and AFM imaging, energy dispersion x-ray spectroscopy (EDS) as well as four-point probe resistivity measurements.

3. Photochemistry of fabrication solutions

The absorption process for silver cations has been reported in literature. The formation of silver sedimentation upon irradiation of silver ion containing solutions with an 800 nm pulsed femtosecond laser confirmed that such process is indeed a two photon process, as it followed an intensity to the second power dependence [21]. The role of individual chemicals in the process has been explored elsewhere. For instance, Jiang and coworkers demonstrated that citric acid serves as a relatively weak binding ligand, and a kinetically slow reducing agent for the formation of silver atoms [22]. The slow kinetics of the reduction process makes citric acid an excellent choice of reducing agent for the controlled photoreduction of silver ions, which is itself an autocatalytic process [23]. The weak acidity of citric acid, which diminishes its binding to silver cations, can be overcome using a salt (e.g., trisodium citrate) as it readily ionizes in aqueous solution. Further addition of surfactants are also necessary for the controlled reduction as citrate anions are very weak stabilizers. Finally, the presence of aqueous NH3, results in the formation of 'Tollen's reagent' {[Ag(NH3)2]+} *in situ*, which is active towards reduction in presence of reagents like citric acid. As depicted in figure 2, the net stoichiometry of the reaction is dependent on multiple species, with a net photoreduction of silver cations coupled with the oxidation of citrate anions.

In order to determine the differences in the light absorption properties of the fabrication solutions containing different protective agents, various combinations of DSIs, trisodium citrate, and NLSS were analyzed using UV–vis absorption spectroscopy. Figure 1 compares the absorption spectra obtained ~1 h after sample preparation and 4 d after sample preparation. Over a period of 4 d (in the dark) a large absorption peak centered at $\lambda = 450$ nm forms in the solution containing DSI, trisodium citrate, and NLSS, indicating the presence of silver nanoparticles. Because these solutions were kept in the dark, the complex that forms when DSI, citrate, and NLSS are all in solution causes the chemical reduction of the DSI without external energy input. On the other hand, the solution containing DSI did not show any evidence of silver reduction over 4 d, while the DSI + citrate solution reduced a small amount of silver and the DSI + NLSS solution reduced a slightly larger amount. Thus, it is clear that all of the components are required for the creation of the reduced silver species without the addition of incoming radiation. These results also give evidence to the hypothesis that this is a two-photon absorption process, because the absorption of all solutions is negligible at the incident radiation wavelength of 800 nm. In addition, these results elucidate the time dependence of fabrication solutions which needs to be accounted for during fabrication.

Cyclic voltammetry data of NLSS in a water solution demonstrated that the surfactant was redox-inactive and only acts as a stabilizing agent. That is, a sweep across the electrochemically accessible window of the aqueous solution showed that NLSS was incapable of either accepting or donating electron, and this is consistent with previous reports

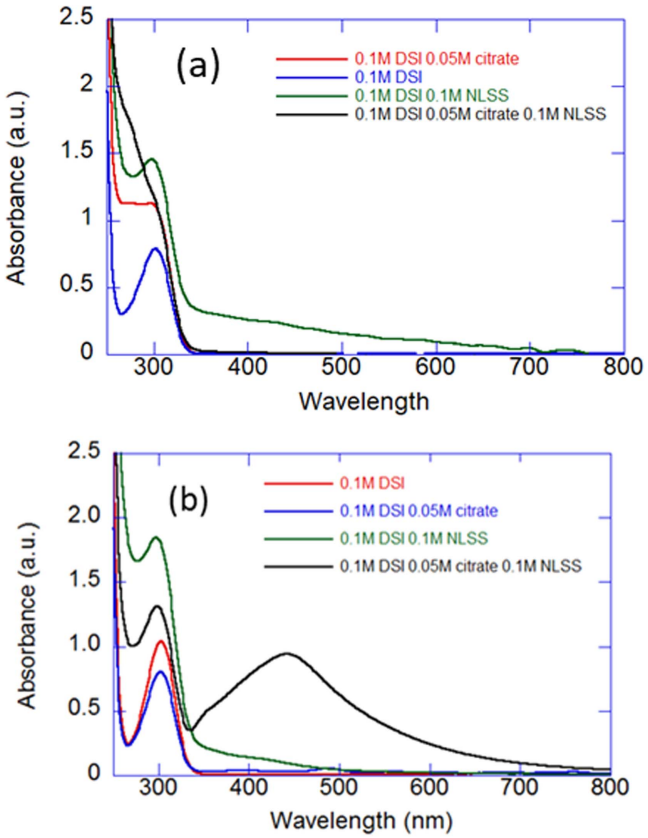

Figure 1. UV–vis absorption spectra of the silver nanofabrication solutions (a) 1 h and (b) four days after the initial mixing of the solutions. The large peak at 450 nm seen in (b) indicates a large amount of silver nanoparticles that have been formed in solution.

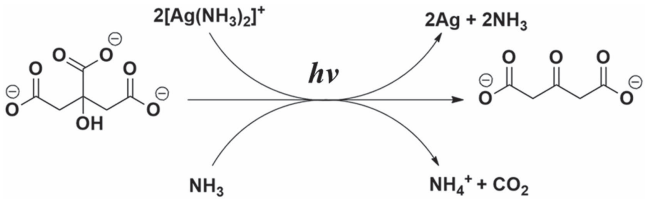

Figure 2. Schematic of the photoreduction process.

of the associated electrochemistry [24, 25]. Moreover, this is in agreement with the idea that citrate is the only reducing agent present in the fabrication solutions. Although the pristine NLSS does not act as a reducing agent as an isolate species, the absorption spectrum in figure 1(b) indicates that the complex that forms in a DSI + NLSS solution reduces the threshold for the silver reduction process by water oxidation. Because NLSS does not participate in the reduction reaction, the reduction of silver ions in solutions of DSI + citrate and DSI + citrate + NLSS can be expressed by the scheme depicted in figure 2.

These studies regarding the photochemistry of the silver ion fabrication solutions revealed the roles of each of the added chemicals and provides guidance on how the chemicals and laser parameters should be optimized. The results of the manufacturing of nanostructures using these solutions will be discussed next.

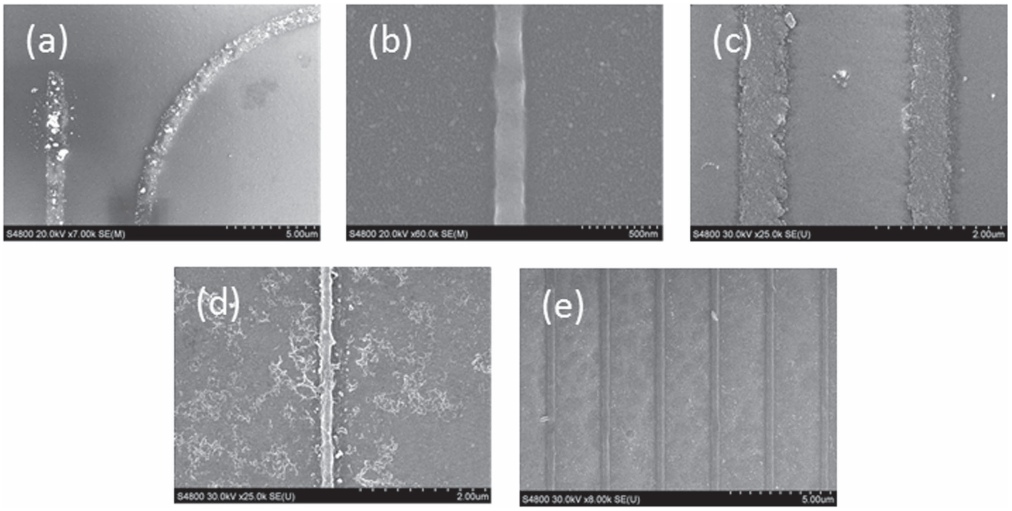

Figure 3. SEM images of silver nanowires fabricated using various combinations of DSI, citrate, and NLSS. (a) Silver wire and circle fabricated using $AgNO_3$ with a laser fluence of 0.66 J cm^{-2} scanned at 5 μm s^{-1}. (b) Silver wire fabricated using DSI + NLSS with 0.086 J cm^{-2} laser power scanned at 7.5 μm s^{-1}. (c) Silver wires fabricated using DSI + citrate with 0.01 J cm^{-2} laser power scanned at 5 μm s^{-1}. (d) Silver wire fabricated using DSI + citrate + NLSS with 0.05 J cm^{-2} laser power scanned at 6.5 μm s^{-1}. (e) Silver wires fabricated using DSI + citrate + NLSS with 0.05 J cm^{-2} laser power scanned at 5 μm s^{-1}. By adding a protective agent into the silver ion solution, the widths of the silver wires were reduced significantly. Solutions that contained NLSS produced the narrowest and smoothest silver wires.

4. Fabrication of wires and two-dimensional structures

After establishing the photochemistry associated with the complex reaction solutions, the solutions were used to fabricate silver nanowires in order to generate high-resolution, smooth structures with useful electronic properties. SEM images of representative nanowires are shown in figure 3, and the optimized parameters associated with the laser-based fabrication protocol are detailed in the figure caption. In a baseline experiment, wires were fabricated using a solution of aqueous $AgNO_3$. These structures had a large surface roughness and submicron resolution was not achieved (figure 3(a)); this is consistent with a previous report [16]. When a solution of DSI + NLSS was used, the fabricated wires had a much smoother surface and a resolution of 200 nm was achieved (figure 3(b)). This can be explained by the fact that NLSS acts as a protective agent, which reduces the amount of autocatalytic silver reduction and confines the agglomerated silver to a smaller region. Wires fabricated using DSI + citrate had 400 nm minimum linewidth and had a rougher surface as well as rougher edges compared to those fabricated with DSI + NLSS (figure 3(c)). The smallest linewidth (i.e., 180 nm) was obtained using a solution of DSI + citrate + NLSS (figure 3(d)). Overall, the quality of these wires was similar to those fabricated using DSI + NLSS, but the solution did not dry out on the substrate as quickly, which allowed for a longer fabrication time when needed. Without the addition of citrate, the fabrication solution dried out within 5 min, which is usually not enough time to fabricate larger, more complicated circuitry. The fabrication solution containing DSI + citrate + NLSS was stable enough to fabricate structures over a period of greater than 2 h. As can be seen in figure 3(e), when NLSS and citrate are both present in the fabrication solution the resulting lines are smooth and continuous with low variability in surface quality across multiple lines. The scanning speeds and incident laser powers were varied in figures 3(a)–(e) to achieve the best results for each combination of chemicals. For fabrication of wires with any combination of chemicals, the optimal laser scan speed range is between 1 and 10 μm s^{-1}. Wires fabricated at speeds faster than this were not continuous enough to give a smooth profile. Using this range of scan speeds, the optimal range of laser fluence for fabricating nanowires was between 0.04 and 0.12 J cm^{-2}. Wires fabricated with laser fluences above this range had large unwanted silver particles reduced, which resulted in very rough surfaces and wires fabricated with laser fluences below this range did not form continuous structures. It was observed that no combination of laser scan speed and fluence gave smooth lines when using DSI + citrate fabrication solution, and the narrowest, smoothest lines were fabricated with DSI + NLSS or DSI + citrate + NLSS. Figure 3(d) showed another aspect of the fabrication, that the fabricated wire needs to be rinsed in the fabrication solution before being rinsed in water, otherwise the substrate would appear to be dirty (for all other images, the fabricated sample were rinsed in solution and water).

Because the electronic properties of the fabricated nanostructures are critical to the end applications of these materials, resistivity measurements of the nanowires were performed using the 4-point probe technique. Gold contact pads were fabricated on a glass substrate first and then silver wires were fabricated across the pads, allowing for resistance measurements to be made in a ready manner. The resistivity values were evaluated from the measured resistance, the cross-sectional area of the wires obtained from AFM measurements, and the length of the wires. The average resistivity value for (four) wires fabricated

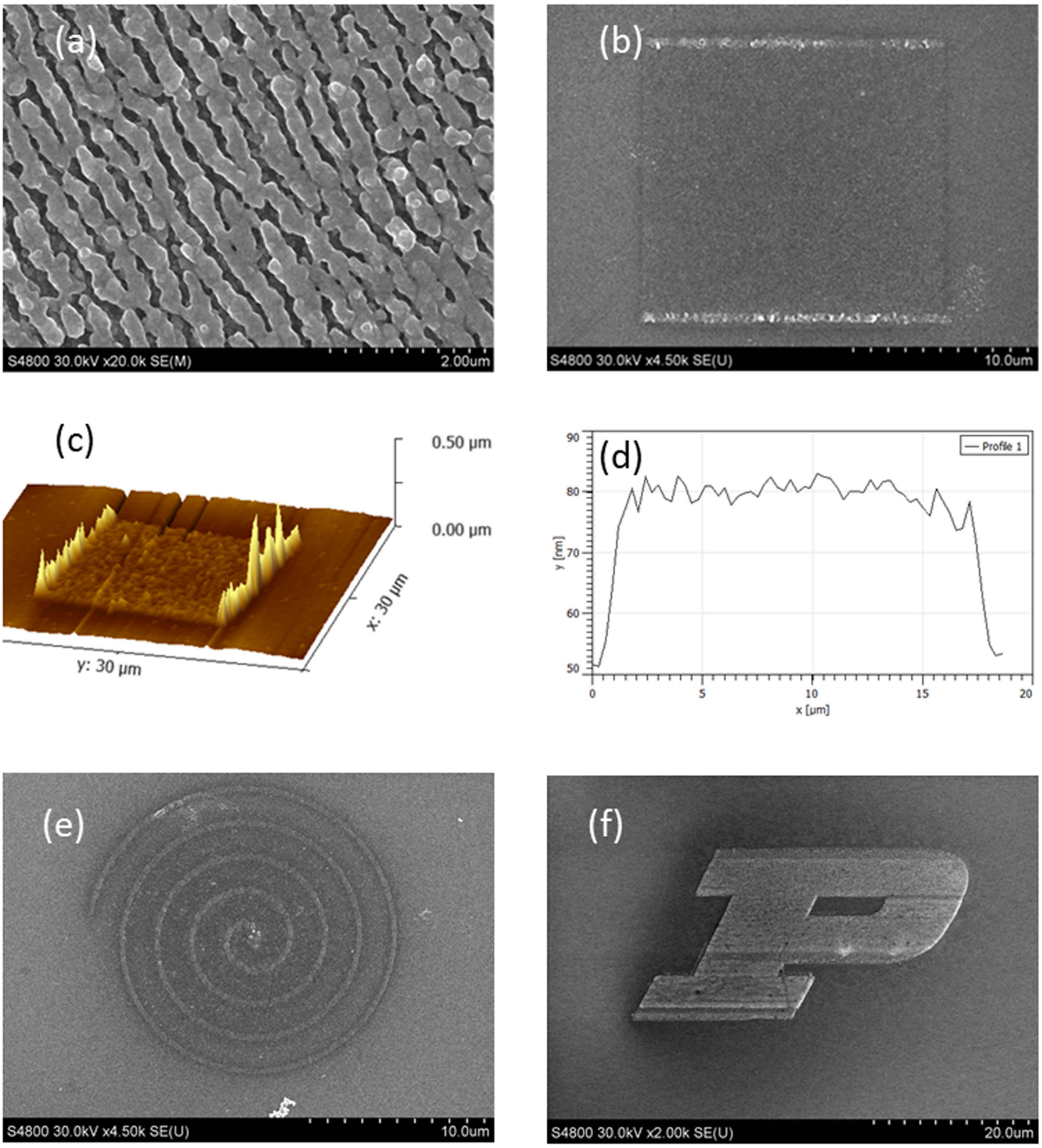

Figure 4. (a) SEM image of laser induced periodic surface structure (LIPSS) fabricated when the laser focal spot was scanned at the substrate surface with a laser power of 0.11 J cm^{-2} scanned at 10 $\mu m\ s^{-1}$. (b) SEM image of smooth square pad fabricated when laser focal spot was scanned slightly below the substrate surface with a laser power of 0.26 J cm^{-2} scanned at 100 $\mu m\ s^{-1}$. (c) Three-dimensional AFM image of square pad seen in (b). (d) AFM cross-sectional scan of the square pad seen in (b). (e) SEM image of spiral structure fabricated using this method with a laser power of 0.26 J cm^{-2} scanned at 20 $\mu m\ s^{-1}$. (f) Purdue P logo fabricated using this method with a laser power of 0.26 J cm^{-2} scanned at 100 $\mu m\ s^{-1}$.

using DSI + citrate was $4.35 \times 10^{-6}\ \Omega$ m which is 273× the value of bulk silver, the average resistivity value of wires fabricated using DSI + NLSS was $1.29 \times 10^{-5}\ \Omega$ m, which is 773× the value of bulk silver, and the average resisitivity value of wires fabricated using DSI + NLSS + Citrate was 2.39×10^{-6} which is 151× the value of bulk silver. In order to reduce the resistivity of the nanowires, the samples were thermally annealed in a nitrogen environment at 300 °C for 20 min. The resistivity values for wires after annealing were $1.79 \times 10^{-7}\ \Omega$ m for those fabricated with DSI + citrate, which

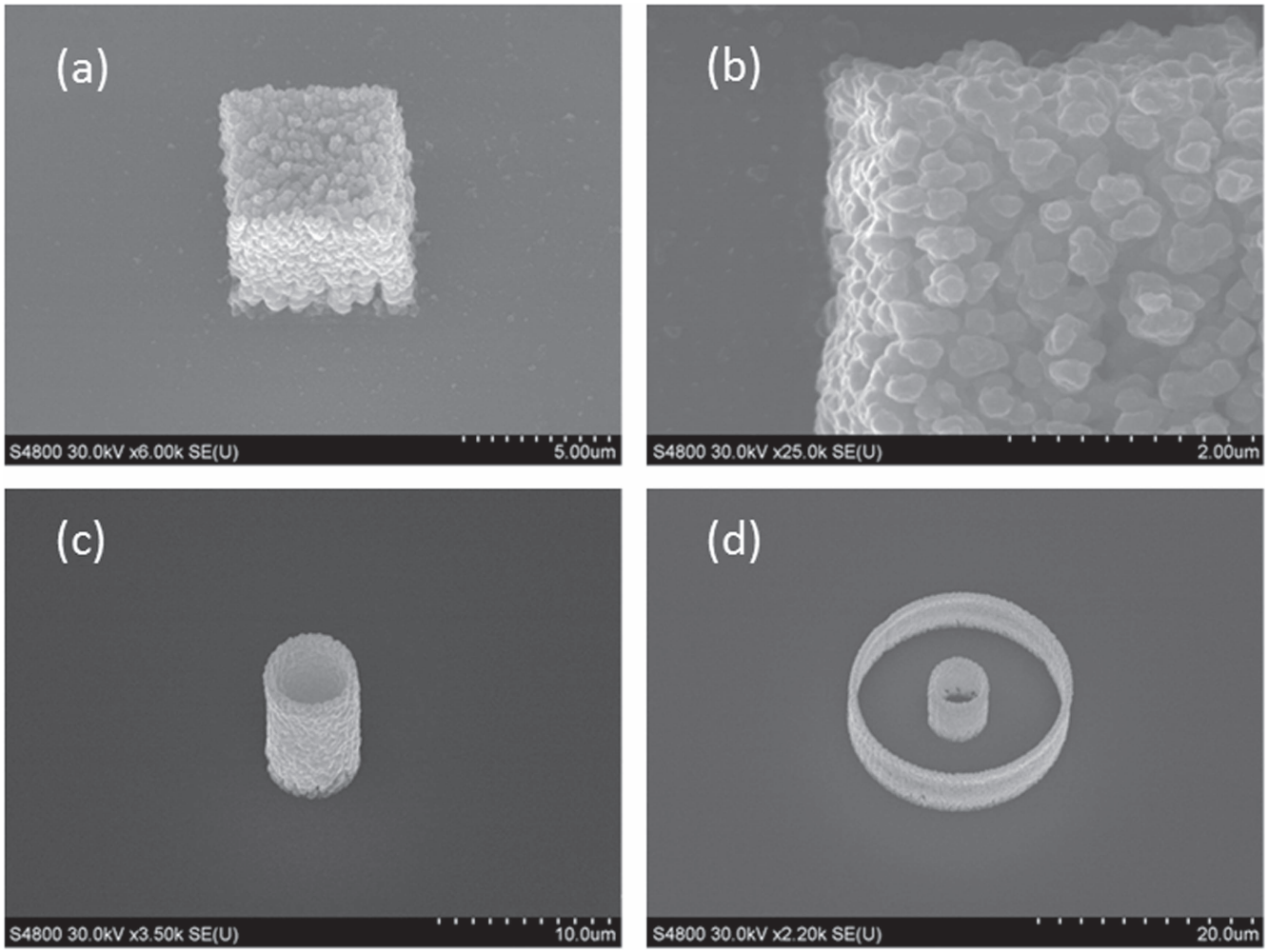

Figure 5. Three-dimensional silver structures fabricated with 0.1 M DSI + 0.1 M NLSS + 0,05 M citrate. (a) SEM image of 5 μm cube fabricated with a laser power of 0.26 J cm^{-2} for the first layer and 0.19 J cm^{-2} for subsequent layers with a scanning rate of 100 μm s^{-1}. (b) Higher magnification SEM image of the cube seen in (a) showing its density, sharp corners and a surface roughness/grain size of 200 nm. (c) SEM image of fabricated cylindrical shell with 10 μm height and 500 nm thickness fabricated with a laser power of 0.14 J cm^{-2} and a scanning rate of 50 μm s^{-1}. (d) SEM image of 5 μm tall concentric cylindrical shells fabricated with a laser power of 0.14 J cm^{-2} and a scanning rate of 50 μm s^{-1}.

is 11× that of bulk silver, 1.06 × 10^{-7} Ω m for those fabricated with DSI + NLSS, which is about 7× that of bulk silver, and 6.46 × 10^{-8} for those fabricated with DSI + NLSS + Citrate which is about 4× that of bulk silver. All 4 probe resistivity measurements were performed using the same piece of equipment. This is a significant improvement in the resistivity of submicron silver nanowires fabricated using this method; previously the best resistivity achieved was 10× that of bulk silver [20]. It was concluded that for electrical applications, silver nanowires fabricated using this method should be thermally annealed after fabrication in order to remove the residual insulating materials that are present in the fabrication bath. It is also noticed that the resistivity of fabricated nanowires degrades (increases) over time (over a week). Therefore, if one intends to use nanowires as electrical conductor, the surface of the nanowires needs to be coated with a protective layer. EDS measurements showed that the structure made had 79.6% of silver by weight.

Fabrication of two-dimensional structures with filled areas requires different laser parameters because the incident radiation now interacts with the previously deposited silver. When a square pad was scanned with the laser focal spot at the substrate surface, a discontinuous periodic structure was observed (figure 4(a)), and the minimum separation distance (i.e., peak-to-peak distance) was 400 nm. This suggests that adjacent silver nanostructures previously written may interact with the laser beam and cause the formation of laser induced periodic surface structures (LIPSS). For metal and absorbing semiconductors, LIPSS is formed by the interference between the surface plasmon polariton and the incident radiation [26]. By lowering the focal spot slightly into the substrate, the resulting square pad appeared as a much smoother element. This is because the aforementioned interference for forming LIPSS is less likely to occur. The average surface roughness for a two-dimensional structure fabricated using this technique was 7 nm at a silver

thickness of 30 nm, which can be seen in figures 4(b)–(d). The roughness value is in good agreement with the line roughness measurement of silver nanowires which was found to be 7.8 nm. Using this method, the flexibility of two-dimensional patterning was shown by fabricating a spiral and a Purdue University P logo, which are seen in figures 4(e), (f). The optimal laser scan speed range for fabricating 2D structures (with filled in areas) is between 75 and 125 μm s^{-1}, and the optimal laser fluence range is between 0.2 and 0.3 J cm^{-2}. When structures are fabricated at speeds lower than this, the LIPSS phenomenon occurs as is seen in figure 4(a), and speeds higher than this range produce structures that are not continuous. At fluences higher than this range, the LIPSS phenomenon is observed again, while fluences lower than this range produce structures that are not continuous.

5. Fabrication of 2.5-dimensional structures

In addition to the high-resolution two-dimensional structures, this materials combination and deposition method is also capable of allowing for the fabrication of 2.5-dimensional silver structures. Starting with a smooth square pad, similar to that seen in figure 4(b), a 5 μm cube was fabricated by raising the focal point by 100 nm between scanning subsequent layers (figure 5). Because of the LIPSS that form while scanning the laser at the substrate surface and at the surface of previously deposited silver, it was observed that in order to fabricate solid cubes with small grain sizes, the scan direction needed to alternate from vertical to horizontal after each layer in order to rotate the LIPSS orientation which then fills any residual gaps present in the previous layer. The laser power needed to be decreased from 0.26 to 0.19 J cm^{-2} after the first layer was fabricated because absorption of photons by the deposited silver is stronger than two-photon absorption. The resulting cube was solid, had sharp corners and a surface roughness/grain size of ~200 nm. Cylindrical shell structures were fabricated starting from circles with a z step of 100 nm between them and can be seen in figures 5(c), (d). The optimal laser parameter range for fabricating the first layer of a 2.5D structure is the same as fabricating a 2D structure. When adding subsequent layers, the optimal scan speed is between 75 and 100 μm s^{-1} to produce continuous layers while avoiding the LIPSS phenomenon. The optimal range of laser fluences for additional layers is between 0.15 and 0.2 J cm^{-2} for the same reasons as for fabricating 2D structures. A 10 μm tall shell with 500 nm thickness was fabricated and was stable enough to withstand rinsing with water and drying with nitrogen. This represents the tallest stable silver structure fabricated with this method. Concentric cylindrical shells of 5 μm height were also fabricated with 500 nm thickness. The approximate surface roughness for all 2.5-dimensional structures fabricated was 200 nm. These examples demonstrated that stable, high aspect ratio 2.5D structures can be fabricated using this method. This shows a significant increase in the size of nanostructures fabricated with this method compared to previous reports, both in height and area while still maintaining sub-micron feature sizes. Future work will include fabricating more complex three-dimensional structures.

6. Conclusion

Fabrication of two- and three-dimensional silver nanostructures using two-photon reduction of silver ions in a liquid solution was demonstrated. Compared to previous reports using this method: (1) the resistivity of fabricated submicron silver nanowires was reduced to 4× that of bulk silver; (2) smooth two-dimensional patterns with 7 nm surface roughness were generated; and (3) solid cubes as well as 10 μm tall structures with an aspect ratio of 20 were fabricated. While more investigations need to be performed to further reduce the surface roughness of fabricated 2.5-dimensional structures, this report importantly demonstrates that mechanically stable, tall silver structures with high aspect ratios can be fabricated using two-photon reduction in a liquid solution. Future work will also include fabrication of truly three-dimensional structures. This, in turn, provides a key option for fabricating functional structures for applications in electronics and plasmonics.

Acknowledgments

We gratefully thank the National Science Foundation (NSF) for providing support through the Scalable Nanomanufacturing Program (Award Number: 1634832, Program Manager: Dr Khershed Cooper). The authors also thank Prabhukumar Venuthurumilli for help in fabricating contact pads for the electrical measurements.

ORCID iDs

Xianfan Xu https://orcid.org/0000-0003-0580-4625

References

[1] Maruo S, Nakamura O and Kawata S 1997 *Opt. Lett.* **22** 132
[2] Kawata S, Sun H B, Tanaka T and Takada K 2001 *Nature* **412** 697
[3] Li L and Fourkas J T 2007 *Mater. Today* **10** 30
[4] Yokoyama S, Nakahama T, Miki H and Mashiko S 2003 *Thin Solid Films* **438–439** 452
[5] Hada H, Yonezawa Y and Kurakake A 1976 *J. Phys. Chem.* **80** 2728
[6] Yonezawa Y, Sato T, Ohno M and Hada H 1987 Photochemical formation of colloidal metals *J. Chem. Soc. Faraday Trans.* I **83** 1559–67
[7] Wu P W, Cheng W, Martini I B, Dunn, Schwartz B J and Yablonovitch E 2000 *Adv. Mater.* **12** 1438
[8] Stellacci F, Bauer C A, Meyer-Friedrichsen T, Wenseleers W, Alain V, Kuebler S M, Pond S J K, Zhang Y, Marder S R and Perry J W 2002 *Adv. Mater.* **14** 194
[9] Baldacchini T, Pons A C, Pons J, LaFratta C N, Fourkas J T, Sun Y and Naughton M J 2005 *Opt. Express* **13** 1275

[10] Maruo S and Saeki T 2008 *Opt. Express* **16** 1174
[11] Shukla S, Furlani E P, Vidal X, Swihart M T and Prasad P N 2010 *Adv. Mater.* **22** 3695
[12] Vurth L, Baldeck P, Stephan O and Vitrant G 2008 *Appl. Phys. Lett.* **92** 171103
[13] Tsutsumi N, Nagata K and Sakai W 2011 *Appl. Phys.* A **103** 421
[14] Nakamura R, Kinashi K, Sakai W and Tsutsumi N 2014 *Chem. Phys. Lett.* **610** 241
[15] Vora K, Kang S Y and Mazur E 2012 *J. Vis. Exp.* **69** 4399
[16] Tanaka T, Ishikawa A and Kawata S 2006 *Appl. Phys. Lett.* **88** 081107
[17] Ishikawa A, Tanaka T and Kawata S 2006 *Appl. Phys. Lett.* **89** 113102
[18] Cao Y Y, Takeyasu N, Tanaka T, Duan X M and Kawata S 2009 *Small* **5** 1144–8
[19] Cao Y and Gu M 2013 *Appl. Phys. Lett.* **103** 213104
[20] Xu B B *et al* 2010 *Small* **6** 1762–6
[21] Ma Z-C, Chen Q-D, Han B, Liu X-Q, Song J-F and Sun H-B 2015 *Sci. Rep.* **5** 17712
[22] Jiang X C, Chen C Y, Chen W M and Yu A B 2010 *Langmuir* **26** 4400–8
[23] Harada M and Katagiri E 2010 *Langmuir* **26** 17896–905
[24] Rusling J and Suib S 1994 *Adv. Mater.* **6** 922
[25] Zoski C 2007 *Handbook of Electrochemistry* 1st edn (Amsterdam, Boston: Elsevier)
[26] Mitchell J, Zhou N, Nam W, Traverso L and Xu X 2014 *Sci. Rep.* **4** 3908